Nanoscale

Accepted Manuscript

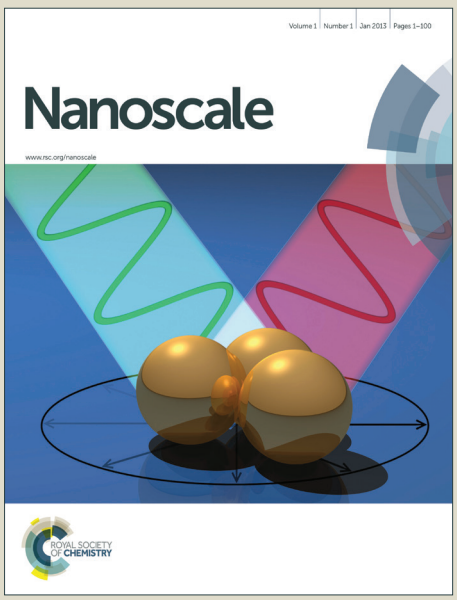

ROYAL SOCIETY OF CHEMISTRY

www.rsc.org/nanoscale

RSC Nanoscale

RSCPublishing

ARTICLE

Carbon Dots obtained using hydrothermal treatment of formaldehyde. Cell imaging *in-vitro*

Cite this: DOI: 10.1039/xoxxoooooox

M. Algarra,[a,*] M. Pérez-Martín,[b] M. Cifuentes-Rueda,[b,c] J. Jiménez-Jiménez, [a] J. C. G. Esteves da Silva,[d] T. J Bandosz,[e] E. Rodríguez-Castellón,[a] J. T. López-Navarrete [f] and J. Casado [f]

Received ooth January 2012,
Accepted ooth January 2012

DOI: 10.1039/xoxxoooooox

www.rsc.org/

Highly photoluminescent carbon dots have been prepared in one step procedure by hydrothermal treatment of formaldehyde at 180 ºC. They show green fluorescence under UV light exposure and emission spectra are centered at 440 nm. Fluorescence lifetimes comprise between 0.7 - 2.70 ns, when the synthesis process lasted 1-7 days. TEM images of nanoparticles showed a homogeneous size/shape distribution. When the thermal treatment process was carried out for a long time (30 days) a formation of aggregates occurred. Carbon dots were further analyzed using ^{1}H and ^{13}C-NMR, Raman and FTIR spectroscopies and XPS. Such nanoparticles showed cell imaging by using mouse MC3T3-E1 pre-osteoblasts as model. The nanoparticles were selectively localized in the cytoplasm without further functionalization and could be realized by cellular phagocytosis, so that the fluorescence of these can be used for living cell imaging *in-vitro*.

Introduction

Carbon dots (CDs) have generated a great interest because of their superior water solubility, chemical inertness, low toxicity, easiness of functionalization, and resistance to photo-bleaching.[1] CDs are usually composed of nanometre-sized sp^2 hybridized graphitic cores and carbonyl surface moieties. Owing to their low cost, low toxicity, biocompatibility, and reasonable photoluminescence, CDs offer an alternative to replace traditional semiconductor quantum dots.[2-5] Additionally, CDs show size dependent photoluminescence and upconversion luminescence properties due to multiphoton processes, which would eventually lead to anti-Stokes type emission.[6,7]

The syntheses of various functionalized and non-functionalized CDs are very well established. Such methods as microwave irradiation,[8-10] combustion of carbon soot,[11,12] activated carbon,[13] carbon xerogel,[14] and laser ablation of graphite[15,16] or thermal degradation/oxidation of suitable molecular precursor such as polysaccharides have been applied.[17,18] The latter method is considered as a one-step procedure, which makes it cost efficient and thus attractive. Application of this procedure leads to oxygen functionalized CDs with a good control of size, shape, and physical properties. These nanoparticles are referred in the literature as carbogenic nanoparticles because of their oxygen content.19 Important feature of these CDs is their hydrophilic character, which makes them suitable for bioimaging, biosensing and photocatalyst applications.[20-23] CDs are also potential replacements for the conventional cadmium and selenium based quantum dots used in biological imaging in vitro and in vivo.[24-29] The objective of this paper is to introduce a new simple synthesis route for CDs based on hydrothermal treatment of formaldehyde. According the state of the art is the first attempt to obtain CDs and presenting a novelty in this nanochemistry field. Also, the mechanism proposed is on full dehydration reaction leading to the formation of carbon nanoparticles. With the use of formaldehyde, is the lowest possible source of CDs and generalizes the use of any carbohydrate as precursor of CDs nanoparticles by dehydration reaction**.** Characterization of these CDs and establishing a relation between their fluorescence emission and functional groups formed on the surface is a targeted research task. Moreover, an important objective is also a demonstration that the obtained CDs, prepared via one-pot hydrothermal process, with excellent water dispersion, have promising in-vitro cell imaging applications.

Results and discussion

The synthetic approach follows the controlled hydrothermal treatment (180 ºC) of formaldehyde for 24 h. After this, CDs are detectable by either DLS or TEM. The TEM images of CDs collected in (Fig. 1a-d) reveal small and spherical particles, with an average diameter <30 nm. Dynamic Light Scattering (DLS) measurements showed that the nanoparticles are well dispersed with an average size (diameter) of 12.50±4.03 nm (Fig. 1e), when analyzed the Fig. 1a which has been used through all the

experiments. For larger period treatments, aggregates with sizes about 200 nm are detected in the samples (Fig. 1b-d). These soluble particles show a negative ζ between -0.025 and -0.078 mV.

To further elucidate the surface features of the CDs, various spectroscopic analyses were carried out. On the FTIR spectra (Fig. 2a) typical bands are seen at 2925 and 2853 cm^{-1}, which corresponded to the stretching vibration of C-H in the group of $-CH_2$.

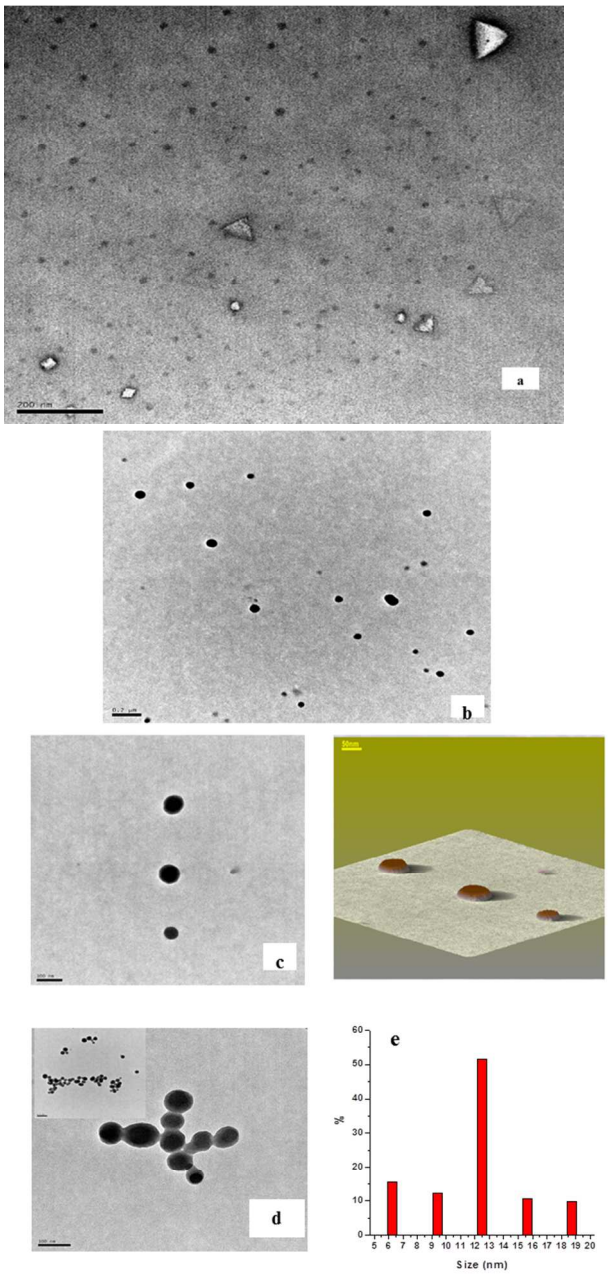

Fig. 1 Representative TEM images of as synthesized CDs showing a homogeneous size/shape distribution **a**) 1 day (200 nm scale bar); **b**) 2 days (200 nm scale bar); **c**) 7 days, inset is a 3d representation of cds (50 nm scale bar), **d**) as well as particle agglomeration after 30 days of thermal treatment process of formaldehyde at 180 ºc, inset is showed other tem image (100 nm scale bar; **e**) size distribution of **a**)

Bands at 1374 and 1448 cm^{-1} respectively are ascribed to the bending of alkyl groups. Broad bands centered at 3361 and 1448 cm^{-1} were ascribed to the stretching vibrations and in-plane bending vibration of -OH, respectively.[30] A band at 1699 cm^{-1} is ascribed to the carbonyl groups (C=O) and, as showed in XPS analysis discussed below, can be attributed to carboxyl functional groups. A band at 1154 cm^{-1} represents the stretching vibrations of C-O. These results suggest that the surface of CDs have methyl groups and their surface is rich in oxygen species.

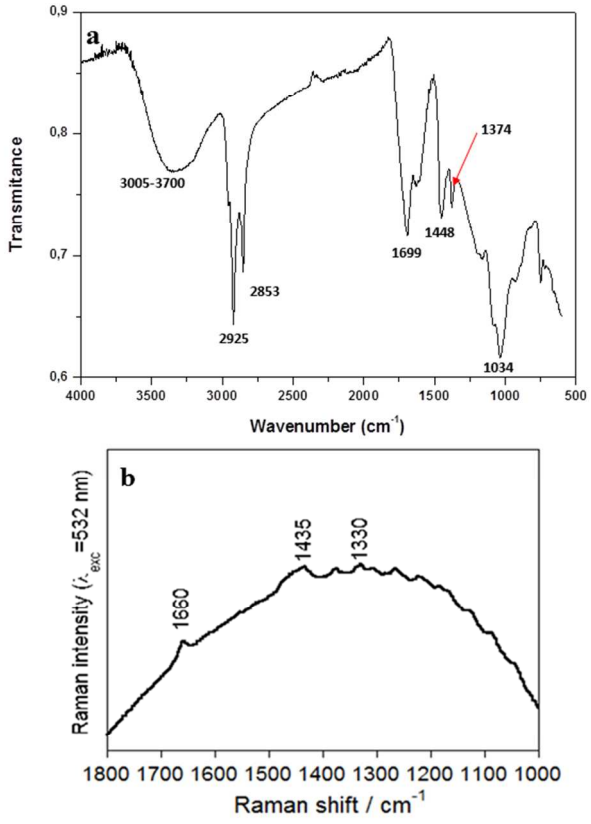

Fig. 2 a) FTIR spectra of CDs and b) Room temperature 532 FT-Raman spectra of CDs

Figure 2b also shows the Raman spectra of the CDs over the high photoluminescence background upon excitation with the 532 nm laser wavelength. The spectrum reveals a clear strong feature at 1660 cm^{-1} associated with the stretching modes of the carbonyl groups of the acidic residues in the carbon dot surface. Typical of the carbon graphitic materials is the presence of the G (≈1600 cm^{-1}) and D (1300-1350 cm^{-1}) bands. We do not observe any Raman signal at 1600 cm^{-1} (G modes), however at the position of the D modes, at 1330 cm^{-1}, a medium intensity signal ascribable to the D band is detected. These spectroscopic fingerprints suggest that the hydrothermal treatment reduces an important fraction of the oxygen groups of the formaldehyde precursor but does not reach a full reduction to sp^2 species. Microcrystalline graphite is also not obtained.

^{1}H-NMR spectrum (*Online supplementary Information Fig SI1*) for the sample obtained after 1 day of treatment show the up-field (1.236 ppm) and down-field (2.153 ppm) singlet peaks which

represent methylene protons of the CDs. The singlet peak at 3.725 ppm is linked to the protons on the *hydroxyl*-methyl group next to hydroxyl group. The peak at 63.70 ppm on ^{13}C-NMR (Fig SI2) spectrum is due to carbons adjacent to hydroxyl groups, and the peak at 29.68 ppm is due to methylene carbons All sample, regardless the synthesis time show the same feature.

The XPS survey spectrum of the CDs particles indicates the presence of carbon (77.37 % atomic concentration), oxygen (22.47% atomic concentration) and negligible amounts of nitrogen and silicon as impurities at the surface. The C1*s* core level spectrum (Figure 3a) can be decomposed in four contributions at 284.8 eV (52%), 286.1 eV (36%), 287.3 eV (8%) and 288.8 eV (4%). The main contribution at low binding energy (284.8 eV) is assigned to the presence of surface methylene group and adventitious carbon. There is a shoulder at 286.1 eV with a high relatively intensity assigned C-OH groups and the other low intensity contributions at 287.3 and 288.8 eV are assigned to C=O and -COO$^-$ moieties, respectively. These results indicate that the surface of CDs is oxidized with a high degree of functionalization. The presence of methylene, alcoholic and carbonyl groups was also detected in the bulk by FT-IR. The O1*s* core level spectrum (Figure 3b) can be decomposed in two contributions at 532.6 eV (92%) and 533.9 eV (8%). The dominant contribution is attributed to oxygen from alcoholic and carbonyl groups, while that at a high binding energy to oxygen from carboxylic groups. The relative intensity of the latter contribution agrees to that found in the C1*s* spectrum (4/(36+8+4) = 8.3 %. The XPS results also indicate that the high degree of functionalization of the surface enables these CDs particles to interact with the surface of many different kinds of solids.

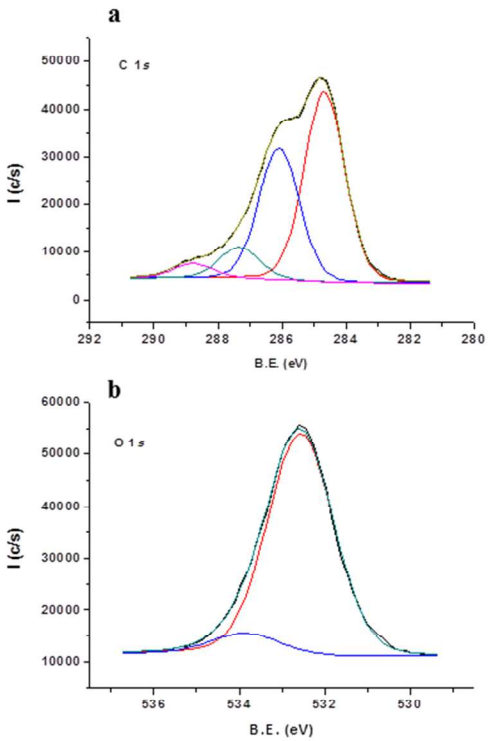

Fig. 3 a) C 1*s* core level spectrum of the CDs sample; **b**) O 1*s* core level spectrum of the CDs sample.

The fluorescence spectra were studied at different excitation wavelengths, in the 325-420 nm range. The highest fluorescence intensity was found at the excitation wavelength of 360 nm with emission maximum at 440 nm. The nature of fluorescence spectra (Fig. 4) suggests that in spite of the different times used in the synthesis process, the CDs nanoparticles exhibit homogeneity in their sizes, as observed by the TEM analysis. The fluorescence spectra for CDs synthesized during 1, 2 and 7 days show an emission band centered at 442 nm, with a shift in the range of 1 nm (Figs. 4a-c). The absence of shoulder in the emission spectra also supports the hypothesis of narrow size distribution of CDs, supporting the TEM image. It is important to mention that CDs aggregation strongly affects the emission spectra (Fig. 4d) and a significant red-shift to 550 nm is noticed. This is corroborated by the strong fluorescence quenching and it is reminiscent of the behavior of conjugated chromophores experiencing aggregation. Interestingly, the aggregation is reversible and when the aggregates are diluted, the solution recovers the emission band at 442 nm (Fig. 4e). This result highlights the reversibility of the supramolecular self-organization of these CDs. This result can be attributed to the concentration effect as a result of supramolecular self-organisation.[31]

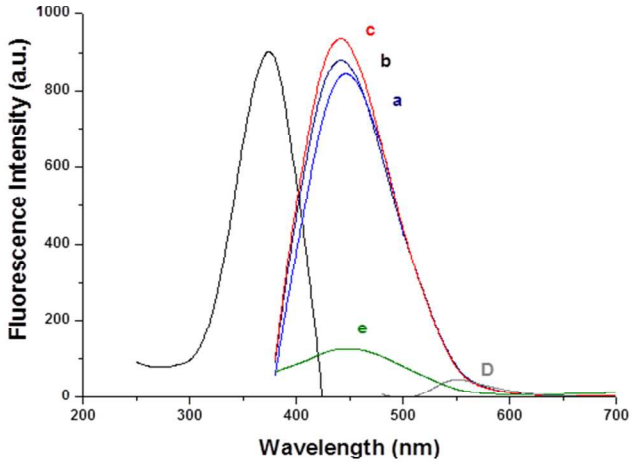

Fig. 4 Fluorescence spectrum of CDs (λ_{ex}= 360 nm): **a**) 1 day; **b**) 2 days; **c**) 7 days (inset the photograph of the dissolution obtained; **d**) 30 days, and **e**) diluted solution of **d**.

Fig. 5 shows the lifetime decay curves of the fluorescence emission, which can be fitted to three kinetics components. The curves are fitted to the selected data after background subtraction for each species and a resultant curve with background is plotted as a red solid line with residues shown above. The measured lifetimes for the different experiments were comprised between 0.7 and 2.70 ns, as showed in Table 1. A three component decay time model resulted in a good fit (χ=1.14). Although the fluorescence lifetime is expected to be sensitive to the different times of thermal treatment, small differences were observed, and the same experimental values were obtained for the CDs obtained in large thermal process. These results, along with the nearly identical spectra, indicate that the surface effects on the emission center of CDs are negligible.

Cell imaging *in-vitro* In order to demonstrate the potential of the synthesized CDs, they were applied directly in the imaging of MC3T3-E1 mouse preosteoblasts cells without any further functionalization. For the control group (0 mg mL^{-1}) a large number of cells could be found in bright field (Fig. 6a). They showed a clear cellular contour and good state and no evident base fluorescence was observed in the corresponding dark field. This result indicates that the cell staining discussed below in the experimental groups was from the fluorescent of the CDs labeled on viable cells, rather than

from base fluorescence. CDs showed excellent staining properties when were used at 0.5 mg mL^{-1}. The same good intensity level was found after 3 to 24 hours of incubation.

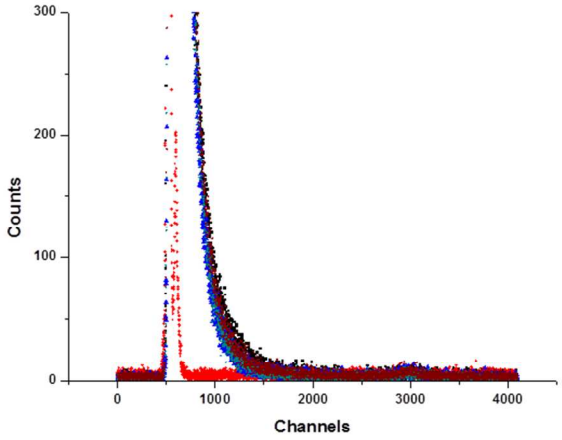

Fig. 5 Fluorescence lifetime curves of CDs obtained by thermal treatment of formaldehyde. A three component exponential-decay curve is fitted to the selected data after background subtraction and the resultant curve with background included is plotted as red.

Table 1. Lifetime intensity decays of formaldehyde CDs

	1 day	2 days	7 days
τ_1 (ns)	0.68 (0.20)	2.76 (0.07)	0.70 (0.03)
τ_2 (ns)	2.98 (0.07)	5.77 (0.03)	3.27 (0.04)
τ_3 (ns)	7.80 (0.08)	7.37 (0.07)	8.90 (0.09)
B_1	0.027 (1.3×10^{-4})	0.028 (1.3×10^{-4})	0.042 (3.1×10^{-4})
B_2	0.045 (3.3×10^{-4})	0.044 (3.7×10^{-4})	0.042 (3.1×10^{-4})
B_3	0.005 (3.2×10^{-5})	0.006 (3.4×10^{-5})	0.027(1.1×10^{-4})
A	7.28 (0.08)	7.49 (0.26)	6.93 (0.22)
χ	1.14	1.23	1.06

The fluorescence was localized as coming from filling the cytoplasm and the nucleus was not marked. Regardless the time of incubation, staining differences were found at different concentrations of CDs (Fig. 6b-d) and 0.1 mg mL^{-1} was found as being extremely-low staining. While cells incubated with 0.5 mg mL^{-1} of CDs for 3 hours before fixation showed an intense fluorescence, no evidence of staining could be observed when the incubation with CDs occurred after the cells were fixed. These results indicate that the CDs could cross the cell membrane and come into the cytoplasm of living cells by endocytosis mechanism. This phenomenon is consistent with the conclusion reported previously where slightly negative ζ of CDs were able to stain selectively the cytoplasm. [32]

Furthermore, the photoluminescence intensity of the stained cells showed no obvious reduction after continuous excitation for more than 1-2 hours, suggesting that CDs possessed a remarkable photostability and low photo-bleaching. These results suggest that the present CDs have promising applications *in vitro* analysis, and can be easily imaged by conventional fluorescence microscopy. The cell viability was tested with Trypan Blue to determine the number of viable cells present in cell culture treated with CDs. Any differences were found between control and the different experimental situations.

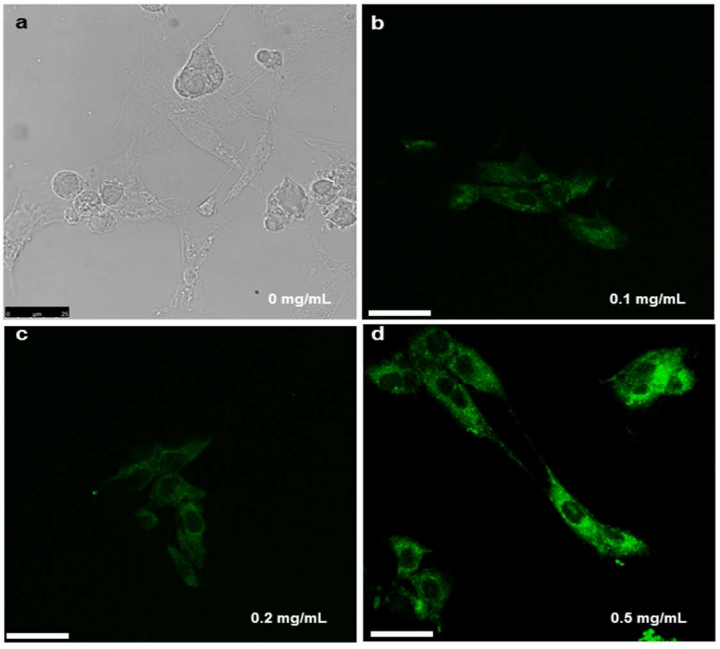

Fig. 6 Confocal images of mouse preosteoblasts treated with different CDs concentrations after 24 hours treatment. **a**) Used as a negative control (bright light); **b-d**) Staining differences were found at different concentrations of CDs, being higher at 0.5 mg mL^{-1} (dark field). Scale: 25 mm.

Experimental

Materials and Methods

Synthesis of CDs Formaldehyde (37%, Sigma-Aldrich, Spain) was used as a CDs precursor. 100 mL were transferred into a 150 mL Teflon lined stainless-steel reactor that was heated at 180 ºC for 1, 2, 7 and 30 days. After completion of the process, the brownish solution was cooled down at room temperature. An excess of acetone was added and the suspension was then centrifuged (10.000 rpm, 15 min). The solution containing the synthesized CDs nanoparticles obtained were evaporated under vacuum.

Characterization and Data Analysis Transmission electron microscopy (TEM) of CDs was performed on a Philips CM-200 by evaporating one drop on carbon coated cooper. Infrared measurements were made with a Bruker Equinox 55 FT-IR spectrometer fitted with a Golden Gate single reflection ATR accessory kit from Specac. All spectra were collected using a resolution of 2 cm^{-1}, 50 scans were collected. Resonance FT-Raman spectra with excitation at 532 nm were recorded on a Senterra Raman Microscope from Bruker. ^{1}H and ^{13}C-NMR spectra were recorded with a 400 MHz ARX 400 Bruker spectrometer by using the residual solvent peak in $CDCl_3$ (δ_H = 7.24 ppm for ^{1}H and δ_C =

77.0 ppm for ^{13}C) or CD_3SOCD_3 (δ_H = 2.50 ppm for 1H and δc = 39.5 ppm for ^{13}C). X-ray photoelectron spectra (XPS) were obtained using a Physical Electronics PHI 5700 spectrometer with a non-monochromatic Al K_α radiation (300 W, 15 kV, hν = 1486.6 eV) as the excitation source. Spectra were recorded at 45º take-off angles by a concentric hemispherical analyzer operating in the constant pass energy mode at 25.9 eV, using a 720 μm diameter analysis area. Under these conditions the Au $4f_{7/2}$ line was recorded with 1.16 eV FWHM at a binding energy of 84.0 eV. The spectrometer energy scale was calibrated using Cu $2p_{3/2}$, Ag $3d_{5/2}$ and Au $4f_{7/2}$ photoelectron lines at 932.7, 368.3 and 84.0 eV, respectively. Charge referencing was done against adventitious carbon (C1s 284.8 eV). Solid surfaces were mounted on a sample holder without an adhesive tape and kept overnight in high vacuum in the preparation chamber before they were transferred to the analysis chamber of the spectrometer. Each region was scanned with several sweeps until a good signal-to-noise ratio was observed. The pressure in the analysis chamber was maintained lower than 10^{-9} Torr. A PHI ACCESS ESCA-V6.0 F software package was used for acquisition data and Multipak supported by MATLAB for data analysis. Spectral decomposition were done using Gaussian-Lorentz curves with similar FWHM values. The accuracy of binding energy (BE) values was within ±0.1 eV. The size and zeta potential (ζ) of CDs were determined using a Zetasizer Nano ZS (Malvern Instruments, U.K.) equipped with a 4 mW HeNe laser operating at λ= 633 nm. All samples were measured at a scattering angle of 173° (for size) and 13º (ζ) and were average of three tests. Size measurements, using dynamic light scattering (DLS), were performed at 25 ºC in a polystyrene cell (ZEN0040). The ζ measurements were also performed at 25ºC in polycarbonate folded capillary cells, incorporated with gold plated electrodes (DTS1060C) and deionized H_2O was the dispersion medium. Both, size and ζ were automatically obtained by the software, using the Stokes-Einstein and the Henry equation, with the Smoluchowski approximation. The fluorescence spectra were studied at different excitation wavelengths, in the 325-420 nm range, recorded with a Horiba Jovin Yvon Fluoromax 4 TCSPC spectrophotometer with an integration time of 0.1 s and a slit of 5 nm. Lifetimes deconvolution analysis (Decay Analysis Software v.6.4.1 (Horiba Jovin Yvon). Fluorescence decays were interpreted in terms of a multi-exponential function: $I(t) = A+\Sigma B_i \exp^{-t/\tau i}$, where A and Bi are the pre-exponential factors and τi the decay times.

In vitro assay for labeling living cells A mouse preosteoblastic cell line, named MC3T3-E1 (ECACC, catalogue number 99072810), was used for this assay. Cells were cultured with Minimum Essential Medium, alpha-modification (alpha MEM; Sigma Aldrich) supplemented with 10% heat inactivated FBS and 1.25 mg L^{-1} amphotericin B, 105 UL^{-1} penicillin, 100 mg L^{-1} streptomycin and 2 mM L-glutamine, at 37 ºC in a humidified atmosphere with 5% CO_2 (standard conditions). Cells were seeded in 24-well plate at a density of 70×10^3 cells mL^{-1} onto poly-L-lysine (0.1 mg mL^{-1}) coated coverslips for cells attachment and cultured for 24 hours in the medium described above. To assess the ability of CDs to mark living cells, the plates were incubated with different CDs concentrations: 0 mg/mL (as a negative control), 0.1, 0.2, and 0.5 mg/mL, for different incubation times: 3, 12 and 24 h. In total 12 experimental conditions, by triplicate. Completed each experimental period, the cells were washed twice with phosphate buffered saline (PBS) and fixed with 4% paraformaldehyde in water. Fluorescence images were acquired using a Leica TCS SP5 II confocal microscope at excitation laser wavelength of 405 nm. To evaluate the ability of CDs to dye fixed cells, plates cultured in the absence of CDs, were fixed with 4% paraformaldehyde and after washing with PBS, incubated with 0.5 mg mL^{-1} solution of CDs for 3 hours. Then, they were washed and the labeling was observed in the confocal microscope.

Conclusions

The results presented in this paper show that formaldehyde can be used as a convenient source for CDs obtained by simple hydrothermal treatment. These CDs exhibit hydrophilic character owing to the abundance of oxygen groups. A long synthesis process increased the nanoparticle size/aggregation and caused red shift on the fluorescence spectra. Therefore as the most promising CDs from the view point of their fluorescence the CVDs synthesized during 1 day were chosen. The cellular localization of CDs was studied in vitro and applied in MC3T3-E1 mouse preosteoblasts cells. The results showed strong fluorescence coming CDs present in a cytoplasm. This phenomenon was linked to the negative values of ζ which follow the nature of some components of the cytoplasm. The results presented can contribute to the advance in cell imaging technique. Moreover, CDs nanoparticles can be used as potential marker of toxic species, for instance heavy atoms, which quenched the fluorescence, when are presented in the cytoplasme.

Acknowledgements

Authors thank to the Spanish Ministry of Economy and Competitively (Project CTQ2012-37925-C03-03) and Andalucía Tech Program from University of Malaga. FEDER funds are acknowledged by support the fluorescence confocal microscopy.

Notes and references

[a] *Departamento de Química Inorgánica, Facultad de Ciencias, Universidad de Málaga, Campus de Teatinos s/n, 29071 Málaga, Spain E-mail: malgarra67@gmail.com*

[b] *Departamento de Biología Celular, Genética y Fisiología, Facultad de Ciencias and Instituto de Investigación Biomédica de Málaga (IBIMA). Universidad de Málaga, Campus de Teatinos s/n, 29071 Málaga, Spain*

[c] *Centro de Investigaciones Biomédicas en Red de Bioingeniería, Biomateriales y Nanomedicina (CIBER-BBN)*

[d] *Centro de Investigação em Química, Departamento de Química e Bioquímica, Faculdade de Ciências da Universidade do Porto, Porto, Portugal*

[e] *Department of Chemistry, the City College of New York. 160 Convent Ave, New York, NY 10031. USA*

[f] *Departamento de Química Física, Facultad de Ciencias, Universidad de Málaga, Campus de Teatinos s/n, 29071 Málaga, Spain*

References

1 Y. P. Sun, B. Zhou, Y. Lin, Wang W, K. A. S. Fernando, P. Pathak, M. J. Meziani, B.A. Harruff, X. Wang, H. Wang, P.G. Luo, H. Yang, M. E. Kose, B. Chen, L. M. Veca and S. Y. Xie, Quantum-sized carbon dots for bright and colorful photoluminescence. *J. Am. Chem. Soc.,* 2006, **128**(4), 7756-7757.

2 W. Kwon and S. W. Rhee, Facile synthesis of graphitic carbon quantum dots with size tunability and uniformity using reverse micelles. *Chem. Commun.,* 2012, **48**(43)**,** 5256-5258.

3 S.N. Baker and G.A. Baker, Luminescent carbon nanodots: emergent nanolights. *Angew. Chem. Int. Ed.* 2010, **49**(38), 6726-6744.

4 P. Anilkumar, X. Wang, L. Cao, S. Sahu, J. H. Liu, P. Wang, K. Korch, K. N. Tackett II, A. Parenzan and Y. P. Sun, Toward quantitatively fluorescent carbon-based "quantum" dots. *Nanoscale*, 2011, **3**, 2023-2027.

5 Y. P. Sun, X. Wang, F. Lu, L. Cao, M. J. Meziani, P. G. Luo, L. Gu and L. M. Veca, Doped carbon nanoparticles as a new platform for highly photoluminescent dots. *J. Phys. Chem. C,* 2008, **112**(47), 18295-18298.

6 P. K. Chu and L. Li, Characterization of amorphous and nanocrystalline carbon films. *Mat. Chem. Phys.* 2006, **96**(2-3), 253-277

7 V. K. A. Sreenivasan, A. V. Zvyagin and E. M. Goldys, Luminescent nanoparticles and their applications in the life sciences. *J. Phys. Condens. Matter*, 2013, **25**(19), 194101.

8 J. Jiang, Y. He, S. Li, H. Cui, Amino acids as the source for producing carbon nanodots: microwave assisted one-step synthesis, intrinsic photoluminescence property and intense chemiluminescence enhancement. *Chem. Commun.,* 2012, **48**, 9634963-6.

9 S. Mitra, S. Chandra, T. Kundu, R. Banerjee, P. Pramanik, A. Goswami. Rapid microwave synthesis of fluorescent hydrophobic carbon dots. *RSC Adv.*, 2012, **2**, 12129-12131.

10 X. Wang, K. Qu, B. Xu J. Ren and X. Qu. Microwave assisted one-step green synthesis of cell-permeable multicolor photoluminescent carbon dots without surface passivation reagents. *J. Mater. Chem.,* 2011, **21**, 2445-2450.

11 X. Zhai, P. Zhang, C. Liu, T. Bai, W. Li, L. Dai and W. Liu, Highly luminescent carbon nanodots by microwave-assisted pyrolysis. *Chem. Commun.,* 2012, **48**(64), 7955-7957.

12 B. Selvi, D. Jagadeesan, B. Suma, G. Nagashankar, M. Arif, K. Balasubramanyam, M. Eswaramoorthy and T. K. Kundu, Intrinsically fluorescent carbon nanospheres as a nuclear targeting vector: Delivery of membrane impermeable molecule to modulate gene expression in vivo. *Nano Lett.*, 2008, **8**(10), 3182-3188.

13 Z. A. Qiao, Y. Wang, Y. Gao, H. Li, T. Dai, Y. Liu and Q. Huo, Commercially activated carbon as the source for producing multicolor photoluminescent carbon dots by chemical oxidation. *Chem. Commun.,* 2010, **46**, 8812-8814.

14 S. Chandra, S. Mitra, D. Laha, S. Bag, P. Das, A. Goswami and P. Pramanik, Fabrication of multi-structure nanocarbons from carbon xerogel: a unique scaffold towards bio-imaging. *Chem. Commun.,* 2011, **47**(30), 8587-8589.

15 L. Cao, X. Wang, M. Meziani, F. Lu, H. Wang, P. Luo, Y. Lin, B. A. Harruff, L. M. Veca, D. Murray, S. Y. Xie and Y. P. Sun, Carbon Dots for Multiphoton Bioimaging. *J. Am. Chem. Soc.* 2007, **129**(37), 11318-11319.

16 H. Gonçalves, P. A. S. Jorge, J. R. A. Fernandes and J. C. G. Esteves da Silva, Hg(II) sensing based on functionalized carbon dots obtained by direct laser ablation. *Sens. Act. B: Chem.,* 2010, **145**(1-2), 702-707.

17 A. B. Bourlinos, A. Stassinopoulos, D, Anglos, R, Zboril, M. Karakassides and E. P. Giannelis, Surface functionalized carbogenic quantum dots. *Small,* 2008, **4**(4), 455-458.

18 M. Algarra, B. B. Campos, K. Radotić, Mutavdžić, T. Bandosz, J. Jiménez-Jiménez, E. Rodriguez-Castellón, J. C. G. Esteves da Silva, Luminescent Carbon Nanoparticles: Effects of chemical Functionalization, and Evaluation of Ag^{+} Sensing properties. J. Mat. Chem A 2014 (In press) DOI:10.1039/C4TA00264D

19 J. T. S. Peng, Simple Aqueous Solution Route to Luminescent Carbogenic Dots from Carbohydrates. *Chem. Mater.,* 2009, **21**(23)**,** 5563-5565.

20 A. B. Bourlinos, R. Zbořil. J Petr, A. Bakandritsos, M. Krysmann, and E. P. Giannelis. Luminescent Surface Quaternized Carbon Dots. *Chem. Mater.*, 2012, **24**(1)6-8.

21 S. T. Yang, X. Wang, H. Wang, F. Lu, P. G. Luo, L. Cao, M. J. Meziani, J. H. Liu, Y. Liu, Y. Huang and Y. P. Sun, Carbon Dots as Nontoxic and High-Performance Fluorescence Imaging Agents. *J. Phys. Chem. C*, 2009, **113**(42), 18110-18114.

22 S. T. Yang, L. Cao, P. G. Luo, F. Lu, F. Wang, H. Wang, M. J. Meziani, Y. Liu, G. Qi and Y.P. Sun, Carbon dots for optical imaging *in vivo. J. Am. Chem. Soc.,* 2009, **131**(32), 11308-9.

23 J. C. G. Esteves da Silva and H. Gonçalves, Analytical and bioanalytical applications of carbon dots. *Trends Anal. Chem.* 2011, **30**(8), 1327-36.

24 H. Li, X. He, Z. Kang, H. Huang, Y. Liu, J. Liu, S. Lian, C. H. A. Tsang, X. Yang and S. T. Lee, Water-soluble fluorescent carbon quantum dots and photocatalyst design. *Angew. Chem. Int. Ed.* 2010, **49**(26), 4430-4434.

25 A. Nagy, J. A. Hollingsworth, B. Hu, A. Steinbruck, P. C. Stark, C. Rios-Valdez, M. Vuyisich, M. H. Stewart, D. H. Atha, B. C. Nelson and R. Iyer, Functionalization-dependent induction of cellular survival pathways by CdSe quantum dots in primary normal human bronchial epithelial cells. *ACS Nano* 2013, **7**(10). 8397-8411.

26 A. C. A. Silva, S.L. Vieira de Deus, M. J. B. Silva and N. O. Dantas, Highly stable luminescence of CdSe magic-sized quantum dots in HeLa cells. *Sens. Act. B: Chem.,* 2014, **191**, 108-114.

27 D. Djikanović, A. Kalauzi, M. Jeremić, J. Xu, M. Mićić, J.D. Whyte, R.M. Leblanc and K. Radotić, Interaction of the CdSe quantum dots with plant cell walls. Colloids and Surfaces B: Biointerfaces, 2012, **91**, 41-47.

28 K. Pathakoti, H. M. Hwang, H. Xu, Z. P. Aguilar and A. Wang, In vitro cytotoxicity of CdSe/ZnS quantum dots with different surface coatings to human keratinocytes HaCaT cells. *J. Environ. Sci.* 2013, 25(1), 163-171.

29 Corazzari, A. Gilardino, S. Dalmazzo, B. Fubini and D. Lovisolo, Localization of CdSe/ZnS quantum dots in the lysosomal acidic compartment of cultured neurons and its impact on viability: Potential role of ion release. *Toxicology in Vitro*, 2013, **27**, 752-759.

30 Q. Wang, F. Ye, T. Fang, W. Niu, P. Liu, and X. Li, Bovine serum albumin-directed synthesis of biocompatible CdSe quantum dots and bacteria labelling. *J. Colloid Interface Sci.* 2011, **355**, 9-14.

31 Q. Wang, F. Ye, T. Fang, W. Niu, P. Liu, X. Min, X. Li and S. Iijima, Helical microtubules of graphitic carbon. *Nature,* 1991, **354**, 56-58.

32 F. Würthner, T.E. Kaiser, C.R. Saha-Möller, J-Aggregates: From serendipitous discovery to supramolecular engineering of functional dye materials. *Angew. Chem. Int. Ed.* 2011, **50**(15), 3376-3410.

